

Source rupture process of the Kocaeli, Turkey, earthquake of August 17, 1999, obtained by joint inversion of near-field data and teleseismic data

Yuji Yagi and Masayuki Kikuchi

Earthquake Research Institute, The University of Tokyo

Abstract. The rupture process of the 1999 Turkey earthquake is examined using both near-field strong motion data and teleseismic body wave data. The derived source parameters are as follows: (strike, dip, slip) = (268°, 86°, 180°), nearly pure strike-slip; the seismic moment, $M_0 = 1.7 \times 10^{20}$ Nm ($M_w = 7.4$); the source duration = 20 sec; the fault length = 70 km; the fault width = 15 km. The rupture process is characterized by an asymmetric bilateral rupture propagation and smooth slip. It consists of two major fault segments, a rupture propagating to the west and a second rupture propagating to the east. The maximum dislocation and the maximum dislocation velocity are 6.3 m and 2.7 m/s, respectively, both found at the former segment. The average dislocation is about 4 m. The extent of the coseismic rupture suggests that a considerable part of the anticipated seismic gap remains unruptured.

1. Introduction

On the morning of August 17, 1999, a devastating earthquake (M_s 7.4) struck northwestern Turkey. More than 15,000 people were killed and more than 20,000 people were injured, mainly by the collapse of buildings. The earthquake information determined by the U.S. Geological Survey is as follows: Origin time = 17/08/99 00:01:40 (UT); epicenter = 40.64°N, 29.83°E; depth = 10 km; surface wave magnitude = 7.4. Figure 1 shows the epicenters of the main shock and the aftershocks within a week.

In this paper, we examine the detailed source rupture process using near-field strong motion records provided by the Earthquake Research Department (ERD) of General Directorate of Disaster Affairs of Turkey and the teleseismic data collected by the Data Management Center of the Incorporated Research Institutions for Seismology (IRIS-DMC). Our special concerns were to determine how far a rupture extends coseismically, whether an anticipated seismic gap with a length of 200 km is filled up by seismic faulting, and how the directivity of rupture propagation can be related to strong ground motion distribution.

2. Data and analysis

We retrieved teleseismic body wave (P- and S- waves) data recorded at IRIS-DMC stations via the Internet. Thirteen components at 11 stations were used in the waveform inversion. The seismograph stations are shown in Figure 2. The data were band-passed between 0.01 and 0.8 Hz and converted into ground displacement with a sampling time of 0.5 sec. We also used 12 components of acceleration data obtained at 9 stations of ERD, shown in Figure 1. The acceleration data at stations close to the surface faults were band-passed between 0.02 and 0.5 Hz and numerically integrated into the ground velocity with a sampling time of 0.2 sec. The other data were band-passed between 0.05 and 0.5 Hz and converted to ground displacement with a sampling time of 0.2 sec. Since the start time of near-field strong

motions is not accurate, we made time corrections so that the observed P- or S-wave arrivals coincide with the theoretical arrival time of P- or S- waves.

Applying a multi-time window inversion to the data, we determined the spatio-temporal distribution of fault slip. We used an inversion code originally given by *Yoshida et al.* [1996] and modified it so that the constraint of smoothness and positivity was imposed on the solution. To determine the smoothness parameter objectively, we adopted the minimum Akaike's Bayesian information criterion (ABIC) [*Akaike*, 1980]. We calculated Green's functions for teleseismic body-waves using *Kikuchi and Kanamori's* [1991] method. Green's functions for near-field ground motion were calculated by the discrete wave number method developed by *Kohketsu* [1985]. We used the standard Jeffreys-Bullen's crustal structure with a thickness of 33 km.

Considering the quality of observed records, we determined their relative weight so that the standard deviations of the near-field data, the far-field P-wave and the far-field S-wave are about 10%, 10% and 20% of their own maximum amplitude, respectively.

We assumed that faulting occurs on a single fault plane and that the slip angle is unchanged during the rupture. We adopted the fault mechanism: (strike, dip, slip) = (268°, 86°, 180°) obtained by teleseismic body wave analysis, as shown in Figure 1, and the hypocenter determined by ERD [latitude = 40.70°N, longitude = 29.91°E, depth = 16km] as an initial break. This fault mechanism is consistent with Centroid Moment Tensor (CMT) determined by Harvard University.

In order to obtain a gross feature as well as some details of the rupture process, we divided the procedure into two steps. In the first step, we took a broad fault area of 250 km x 30 km to get a rough estimation of the rupture area (Figure 1), which we divided into 25 x 3 subfaults, each with an area of 10 km x 10 km. The slip-rate function of each subfault is expanded in a series of 5 triangle functions with a rise time of 2.0 sec. A rupture front velocity is set at 3.2 km/s, which gives the start time of the basis function at each subfault. Through the inversion procedure the effective rupture area was estimated to be 70 km x 15 km.

In the second step, the fault plane was confined to a narrower area of 93.6 km x 21.6 km and divided into 26 x 6 subfaults, each having an area of 3.6 km x 3.6 km. The slip-rate function of each subfault is expanded in a series of 8 triangular functions with a rise time of 1.0 sec.

3. Result

The inversion results are given in Figures 3 and 4. Figure 3 shows the final dislocation distribution, and Figure 4 represents the snapshot of the dislocation every 1 sec. The source rupture process obtained is mainly divided into two episodes. The first is a rupture propagating upward and westward in a fan-shaped manner during the initial 10 sec. It swept over a 20 km fault area along the fault-strike and 15 km along the fault-dip. The average rupture velocity is about 2.5 km/s. The second rupture started 7 sec after the initial break and propagated unilaterally to the east. The rupture reached to about 50 km from the epicenter. The depth extent is about 8 km, nearly constant along the fault-strike. The rupture propagation is very smooth, and the average rupture velocity is about 3.0 km/s. The rupture in this segment looks like a typical unilateral rupture as described by *Haskell* [1964].

The mean source time for a unit of fault area (3.6 km x 3.6 km) to be ruptured is about 5 sec in the western fault segment, while the source time in the eastern fault segment is 4 sec. The source time may consist of the rise time of dislocation

and the rupture propagation time. In the present case the rupture propagation time for a unit of fault area 3.6 km in length is about 1 sec. Therefore the mean rise times in the western and eastern fault segments are estimated to be about 4 sec and 3 sec, respectively.

The maximum slip amounts to 6.3 m at about 10 km west from the hypocenter. The total seismic moment is $M_0 = 1.7 \times 10^{20}$ Nm ($M_w = 7.4$). This value is in good agreement with that of Harvard CMT: 2.1×10^{20} Nm. The total source duration is 20 sec. The average stress drop $= 2.5 \times M_0 / S^{1.5} = 12$ MPa, where we take the fault area $S = 70$ km \times 15 km. This stress drop is significantly larger than the typical stress drop of 3 MPa for inter-plate earthquakes, but close to the typical value 10 MPa for intra-plate earthquakes.

It should be noted in Figure 3 that the aftershocks are likely to occur near the edges of large slip areas. Figure 5 displays a comparison of the observed records (black) with the synthetics (gray). The waveform match is satisfactory except for the up-down component of GYN.

4. Discussion

As shown above, the 1999 Kocaeli earthquake is characterized by a rapid and smooth bilateral rupture. The rupture pattern may affect the distribution of seismic intensity through the directivity. The intensity distribution given by ERD shows that a heavy ground motion area with seismic intensity of VIII - X [on the scale of Medvedev, Kárník, Sponheuer] extended predominantly east and west. This intensity pattern is consistent with that expected from the directivity effect of our bilateral rupture model.

The data also shows that the source process of the Kocaeli earthquake is divided into two major episodes. This feature may be related to a specific fault geometry in the source region. There is an extension jog in the epicentral region [Barka and Kadinsky-Cade, 1988]. We infer that the rupture first started here and propagated along the western fault segment, and then it triggered another rupture on the eastern fault segment which is separated by a few km of jog from the western segment. The rupture propagation toward the east finally stopped at another extension jog, lying about 40 km east from the epicenter. Thus the fault geometry may strongly control the rupture initiation, interaction and termination.

The maximum ground acceleration is 410 gal observed at SKR, 40 km east from the epicenter. This value is rather small, only half of the value observed in various large earthquakes, e.g., 800 gal in the 1995 Kobe, Japan, earthquake and 900 gal in the recent 1999 Chi-Chi, Taiwan, earthquake, while the maximum ground velocity is about 0.8 m/s, comparable to the typical value observed in large earthquakes. The smoothness of rupture propagation is responsible for the ordinary ground velocity but small acceleration in this earthquake.

In order to assess the possibility of a future earthquake in this region, it is crucial to determine the extent of coseismic rupture of this earthquake. This event occurred in a region of 100- to 150-km long seismic gap between the 1967 event (M_w 7.2) and the 1963 event (M 6.3). This gap was first noted by Toksöz *et al.* [1979], and the hazard analysis was later made by Stein *et al.* [1997]. If we neglect the moment release by the 1963 event, the seismic gap is estimated to extend to about 200 km [Barka and Kadinsky-Cade, 1988].

The surface trace of a seismic fault is one of the measures of fault length. In the present case, the surface rupture was observed at the eastern side of the epicenter. The length of the surface trace amounts to nearly 100 km along the Izmit-Sapanca fault zone. In the western side, it is difficult to identify the surface rupture because of the ocean bottom.

Aftershock distribution is another measure of fault dimension. In the present case, aftershock distribution extends 200 km east-west (Figure 1). However, recent studies on the details of moment release distribution show that aftershocks tend to expand into a surrounding area beyond the coseismic rupture area [Mendoza and Hartzell, 1988; King *et al.*, 1994; Yagi *et al.*, 1999].

In the first step of inversion, we took into account the possibility of coseismic slip around 100 km east of the epicenter, but no significant moment-release was obtained there. This result seems to be inconsistent with the surface fault observed around 90 km east of the epicenter. We may think that postseismic slip occurred beyond the eastern end of the coseismic rupture area.

The waveform inversion provides us with direct information about the extent of the coseismic rupture area. Our inversion result strongly suggests that a major rupture is confined to a region between 20 km west and 50 km east of the epicenter. This implies that the western part of the anticipated seismic gap still remains unruptured. Therefore further and more thorough observations such as seismicity monitoring and Global Positioning System (GPS) measurement are needed to assess the possibility of a future earthquake in the western end of the North Anatolian Fault.

Acknowledgments. We express our gratitude to Dr. K. Koketsu and Dr. K. Kudo who provided us with the information of observed data. We also thank Dr. Ross S. Stein and an anonymous reviewer for their critical reviews. This study was partly supported by the Grant-in-Aid for Scientific Research No. 11694056, from the Ministry of Education, Japan. Y. Yagi is a JSPS Research Fellow.

References

- Akaike, H., Likelihood and Bayes procedure, in *Bayesian Statistics*, edited by J. M. Bernardo, M. H. DeGroot, D. V. Lindley, and A. F. M. Smith, pp. 143-166, University Press, Valencia, Spain, 1980.
- Barka, A. and K. Kadinsky-Cade, Strike-slip fault geometry in Turkey and its influence on earthquake activity, *Tectonics*, 7, 663-684, 1988.
- Haskell, N. A., Total energy and energy spectral density of elastic wave radiation from propagating faults, *Bull. Seism. Soc. Am.*, 54, 1811-1841, 1964.
- Kikuchi, M. and H. Kanamori, Inversion of complex body waves-III, *Bull. Seism. Soc. Am.*, 81, 2335-2350, 1991.
- King, G.C.P., R. S. Stein and J. Line, Static stress changes and the triggering of earthquake, *Bull. Seism. Soc. Am.*, 84, 935-953, 1994.
- Kohketsu, K., The extended reflectivity method for synthetic near-field seismograms, *J. Phys. Earth*, 33, 121-131, 1985.
- Mendoza, C., S. H. Hartzell, Aftershock patterns and main shock faulting, *Bull. Seism. Soc. Am.*, 78, 1438-1449, 1988.
- Stein, R. S., A. A. Barka and J. H. Dieterich, Progressive failure on the North Anatolian fault since 1939 by earthquake stress triggering, *Geophys. J. Int.*, 128, 594-604, 1997.
- Toksöz, M., A. F. Shakal and A. J. Michael, Space-time migration of earthquakes along the north Anatolian fault zone and seismic gaps, *Pageoph*, 117, 1258-1270, 1979.
- Yagi, Y., M. Kikuchi, S. Yoshida, T. Sagiya, Comparison of the coseismic rupture with the aftershock distribution in the Hyuganada earthquakes of 1996, *Geophys. Res. Lett.*, 26, 3161-3164, 1999.
- Yoshida, S., K. Koketsu, B. Shibazaki, T. Sagiya, T. Kato, Y. Yoshida, Joint inversion of near- and far-field waveforms and geodetic data for rupture process of the 1995 Kobe earthquake, *J. Phys. Earth*, 44, 437-454, 1996.

Y. Yagi and M. Kikuchi, Earthquake Research Institute, The University of Tokyo, 1-1-1, Yayoi, Bunkyo-ku, Tokyo, 113-0032, Japan.

(e-mail: yuji or kikuchi@eri.u-tokyo.ac.jp)

(Received November 5, 1999; revised April 10, 2000; accepted April 17, 2000.)

YAGI AND KIKUCHI: SOURCE PROCESS OF TURKEY EARTHQUAKE

YAGI AND KIKUCHI: SOURCE PROCESS OF TURKEY EARTHQUAKE

YAGI AND KIKUCHI: SOURCE PROCESS OF TURKEY EARTHQUAKE

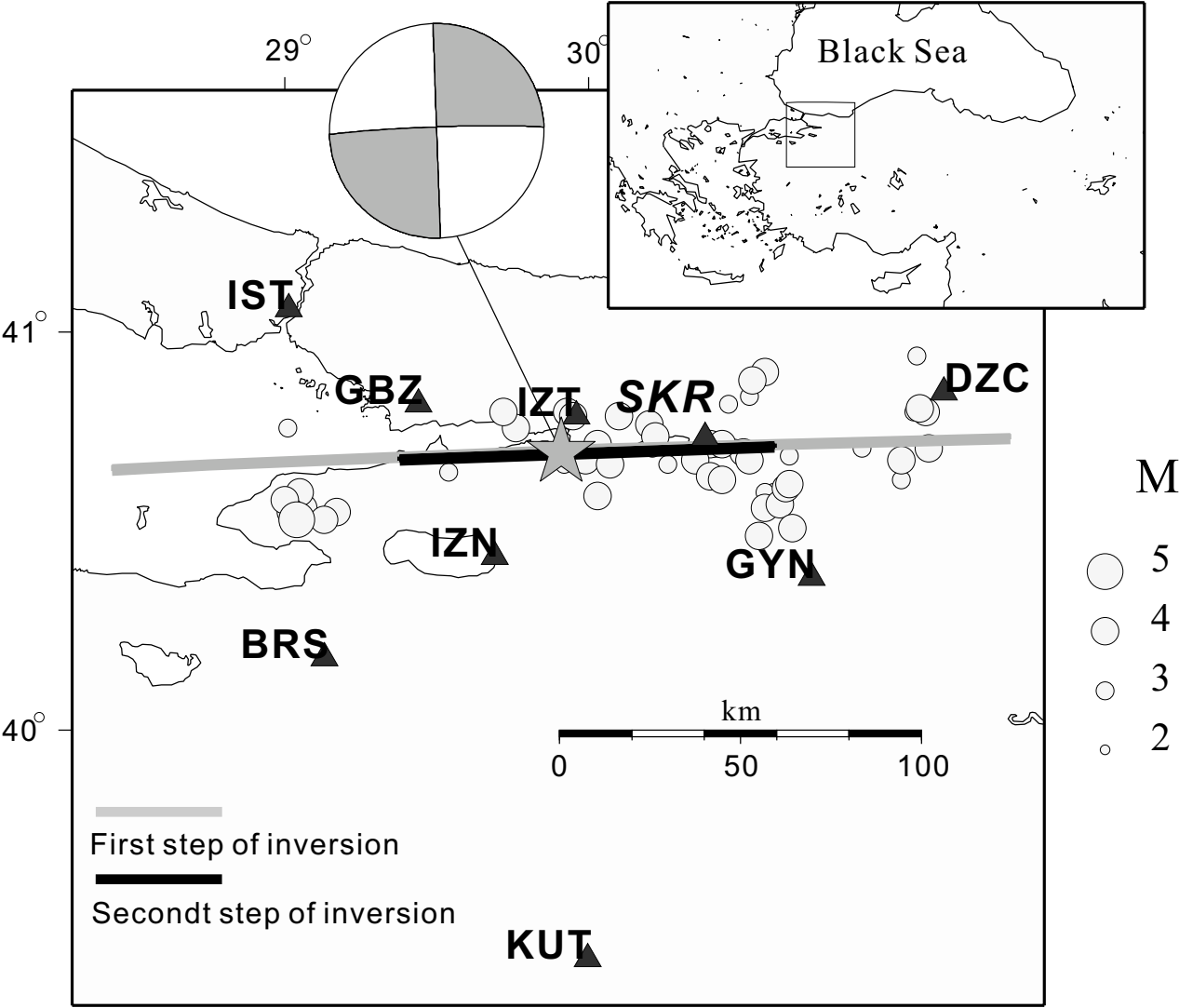
Figure 1. Hypocenter of the main shock (star) and aftershocks (gray circles) determined by the Earthquake Research Department of General Directorate of Disaster Affairs of Turkey. The location of strong motion seismographs used in our analysis is shown by triangles. The focal mechanism is determined in this study. Gray and solid lines represent the extent of the fault plane used in the first step and second step inversions, respectively.

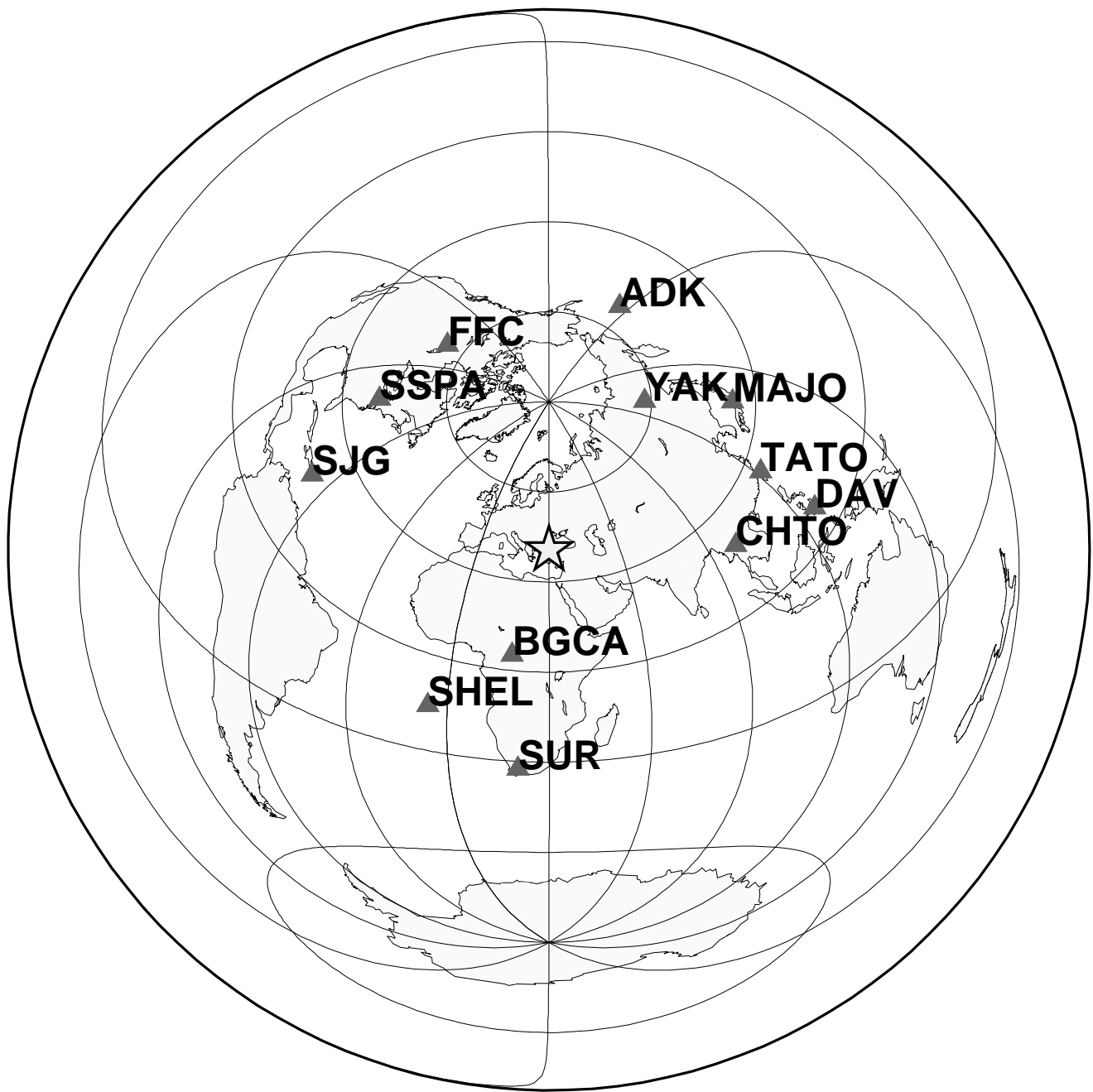
Figure 2. Teleseismic stations used in our inversion. The star represents the epicenter of the main shock.

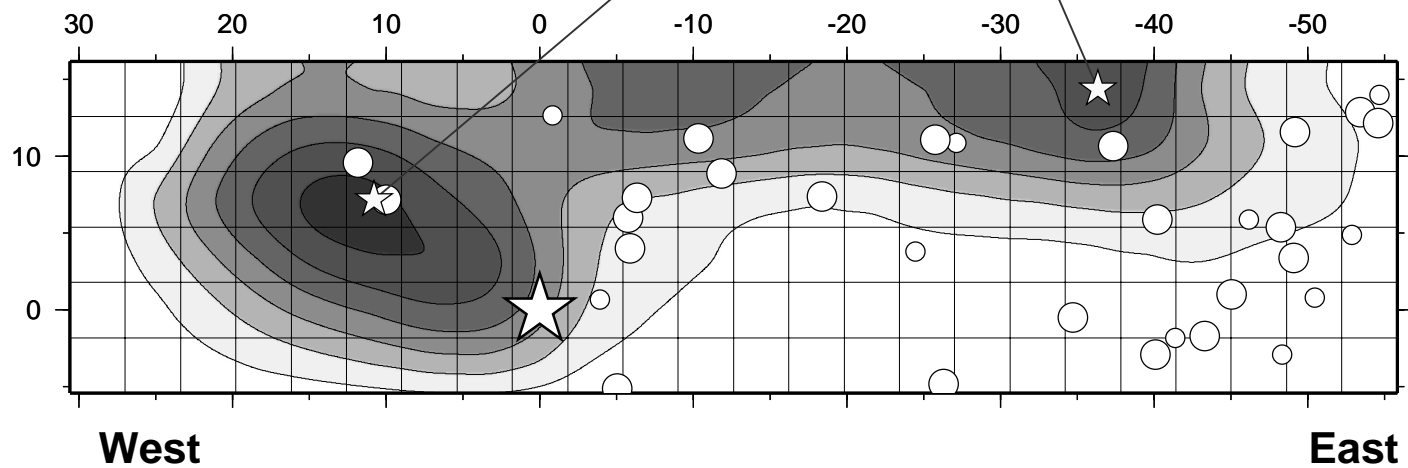
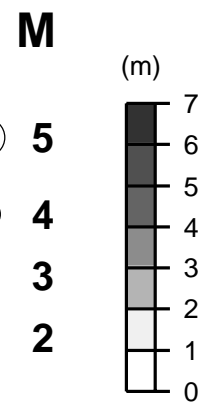
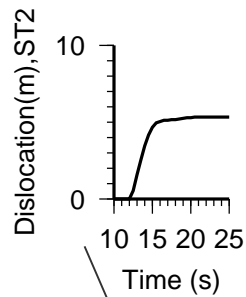
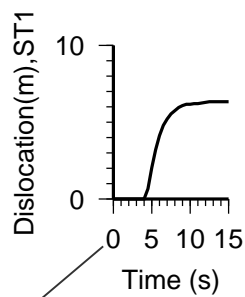
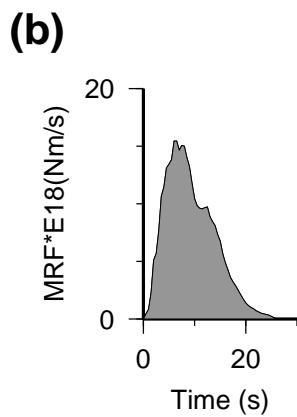
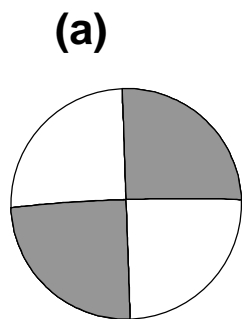
Figure 3. Final results of our joint inversion. (a) Focal mechanism (b) Total moment-rate function. The moment-rate functions for two individual subfault elements are also shown. (c) Distribution of coseismic slip and one-week aftershocks. The star and circles indicate the location of the initial break and of the aftershocks, respectively.

Figure 4. (a) Snapshots of the cumulative dislocation. (b) Snapshots of the interval dislocation.

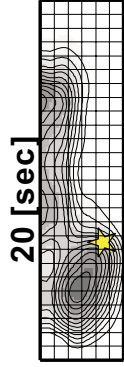
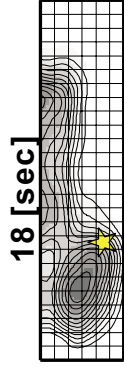
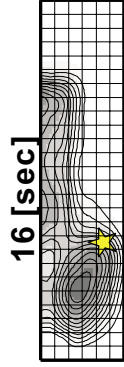
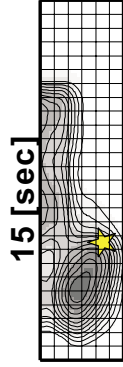
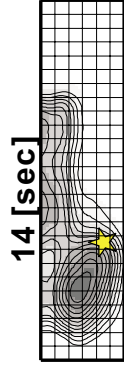
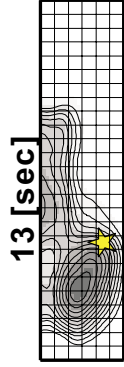
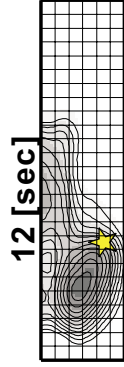
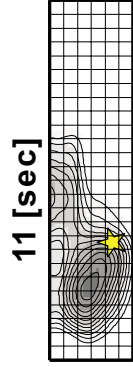
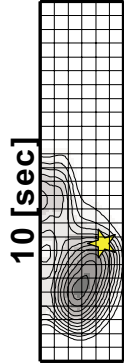
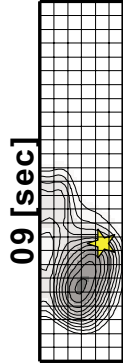
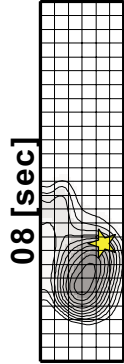
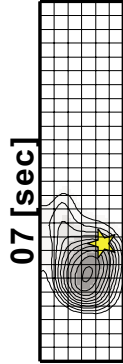
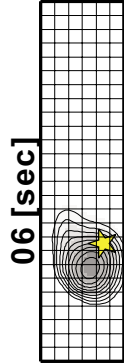
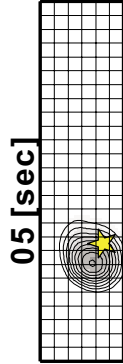
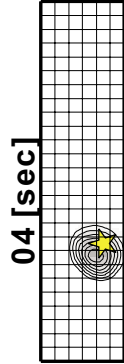
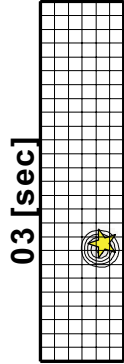
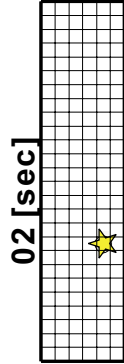
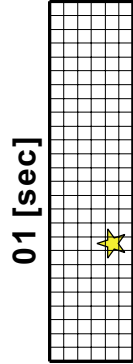
Figure 5. Comparison of the observed waveform (upper trace) with the calculated waveform (lower trace). The numbers below the station code indicate maximum amplitude. (a) Strong motion data (b) Teleseismic body wave data.







(a)



(b)

